Fast-Fourier-Transform Method for Calculation of SAR Distributions in Finely Discretized Inhomogeneous Models of Biological Bodies

DAVID T. BORUP AND OM P. GANDHI, FELLOW, IEEE

Abstract—**The paper describes a novel iterative approach for calculations of specific absorption rate (SAR) distributions in arbitrary, lossy, dielectric bodies. To date, the method has been used for 2-D problems where its accuracy has been confirmed by comparison with the analytic solutions for homogeneous and layered, circular, cylindrical bodies. With computation times that are proportional to $N\log_2 N$ rather than N^2 to N^3 for the method of moments, the present approach should be extendable to 3-D bodies with $N = 10^4$ to 10^5 cells allowing, thereby, details of SAR distributions that are needed for EM hyperthermia, as well as for assessing biological effects.**

I. Introduction

CONSIDERABLE PROGRESS has been made in the last ten years in quantifying whole-body absorption of electromagnetic energy by human and infrahuman models [1], [2]. Whole-body absorption has been obtained for plane-wave irradiation and for cases with simple physical environments, such as the presence of ground and reflecting surfaces in close proximity. On account of complexity and the varied nature of electromagnetic fields in close proximity to a source, only a limited amount of work has been done in quantifying energy doses under near-field conditions of irradiation. Reasonable progress has been made, however, in obtaining mass-normalized rates of energy absorption (specific absorption rates or SAR's) for leakage-type fields, such as those emitted by RF sealers [3] and for simple coupled-type sources, such as dipoles [4], [5]. Advances in dosimetry have had an important role in the formulation of a new frequency-dependent safety standard in Canada [6] and a revised 1982 safety guide [7] recently approved by the American National Standards Institute (ANSI).

Even though much progress has been made in the area of whole-body dosimetry, distributive dosimetry, which is highly relevant to the understanding of biological effects, is in a relatively primitive stage. The method of moments [8], [9] has been used to solve for SAR's in 180- to 340-cell inhomogeneous models of man involving fairly large-size cubic cells with widths on the order of 6–8 cm. Even though the whole-body and even regional values of the SAR's are quite reasonable, individual SAR's for the various locations within the body bear no resemblance to the experimentally determined values. With the method of moments, one solves for the unknown $\vec{E}$-fields (3 components, magnitude and phase) in N cells by solving a large set ($3N \times 3N$ complex) of simultaneous equations, which is quite time-consuming, as computation time increases as N^2 to N^3, and computer storage requirement increasing as N^2.

This paper describes a numerically efficient fast-Fourier-transform (FFT) procedure for calculation of local SAR's in finely discretized inhomogeneous bodies. The method has, to date, been used for 2-D problems, including test cases of homogeneous and layered, lossy, cylindrical bodies for which analytical solutions [10] are available to provide comparisons. With computation times that are proportional to $N\log_2 N$, and with computer-storage requirements proportional to N, the FFT method may be extendable to 3-D bodies with 10 000 to 100 000 cells, allowing thereby extension to higher frequencies as well as to finer detail in SAR calculations than heretofore possible. With the resulting detail, it should be possible to calculate SAR's for the man models in crucial regions, such as the eyes, the gonads, subregions of the CNS, etc., and for rat models the distributions that will allow the experimenters to focus on the exposure conditions in which energy depositions are maximum in the critical organs. A detailed knowledge of the SAR's is also needed to calculate the temperature distribution that plays an important role, not only in assessment of biological hazards, but also in electromagnetic hyperthermia for cancer therapy.

II. Description of the Method

The numerical method presented in this paper is a combination of the K-space method [11] and the method of steepest descents [12]. In this section, the mathematics of the method will be developed for the case of Z-polarized illumination of an arbitrary 2-D dielectric body in the xy plane. Given this geometry, the vector electric-field integral equation simplifies to the scalar integral equation

$$E_z(x, y) = E_z^i(x, y) - \frac{jk_0^2}{4} \int\int_s (\epsilon_{\rho'} - 1) \cdot E_z(x', y') \cdot H_0^{(2)}(k_0 R)\, dx'\, dy' \quad (1)$$

Manuscript received December 29, 1982; revised May 2, 1983. This work was supported in part by NIEHS under Grant ES02304.

The authors are with the Department of Electrical Engineering, University of Utah, Salt Lake City, UT 84112.

0018-9480/84/0400-0355$01.00 ©1984 IEEE

where

E_z the total electric field,
E_z^i the incident electric field,
$\epsilon_{\rho'}$ the complex permittivity of the lossy dielectric at ρ' relative to the permittivity ϵ_0 of free space,
k_0 is the free space propagation constant,
R $|\rho - \rho'|$ ρ = field point position vector, ρ' = source point position vector, and
s surface of 2-D scatterer.

To solve (1), the integral is first discretized into a summation, as in Richmond's moment method [13]

$$E_z(n,m) = E_z^i(n,m) - \frac{jk_0^2}{4}\sum_{i=0}^{N-1}\sum_{j=0}^{M-1}(\epsilon_{ij}-1) \cdot E_z(i,j)\cdot\iint_{\text{cell } ij} H_0^{(2)}(k_0 R_{nm})\,dx'dy' \quad (2)$$

where

$$R_{nm} = \left[(x'-x_{nm})^2 + (y'-y_{nm})^2\right]^{1/2}.$$

The double sum is used, rather than the single sum, of the moment method to preserve the convolutional nature of the equation. The integrals in (2) can be integrated analytically by replacing the square cells with circular cells of equal area. Let

$$K(i-n, j-m) \equiv -\frac{jk_0^2}{4}\iint_{\text{cell } ij} H_0^{(2)}(k_0 R_{nm})\,dx'dy'. \quad (3)$$

Then, (2) becomes

$$E_z(n,m) = E_z^i(n,m) + \sum_{i=0}^{N-1}\sum_{j=0}^{M-1}(\epsilon_{ij}-1)E_z(i,j)K(i-n, j-m). \quad (4)$$

The K-space method is based on the observation that the double sum of the right-hand side of (4) is a 2-D discrete convolution of the sequences $(\epsilon_{ij}-1)E_z(i,j)$ and $K(i,j)$, and therefore can be efficiently computed by use of a 2-D FFT algorithm. Since the FFT method computes a circular, rather than a linear, convolution, the FFT lengths must be chosen as $2N$ and $2M$ to ensure that the convolution is linear inside the dielectric [14]. In effect, this choice of FFT lengths decouples the fields, due to the periodically repeated scatterers introduced by the discrete Fourier transform of the current density. This choice of lengths thus obviates the need for large periods, which would otherwise have restricted the number of cells that could be ascribed to the scattering (biological) body.

The convolution theorem is used to evaluate the sum in (4) in a numerically efficient manner. Clearly, this computation can also be implemented by matrix multiplication by linearly ordering the 2-D sample points (as in the method of moments). This allows (4) to be reformulated as a matrix equation

$$\boldsymbol{E}_z = \boldsymbol{E}_z^i + \vec{\vec{K}}\vec{\vec{D}}\boldsymbol{E}_z \quad (5)$$

where $\vec{\vec{D}}$ is a diagonal matrix containing the dielectric properties and $\vec{\vec{K}}$ is a matrix containing the elements defined in (3). It should be mentioned that the matrix operations indicated in (5) are not implemented by matrix multiplication (an N^2 operation), but by first multiplying the 2-D E_z field by the $(\epsilon_\rho - 1)$ field, and then convolving the resulting current-density field with the 2-D field defined by (3).

In Bojarski's K-space method [11], (5) is solved by the iterative scheme

$$\boldsymbol{E}_z^{\prime(n)} = \boldsymbol{E}_z^i + \vec{\vec{K}}\vec{\vec{D}}\boldsymbol{E}_z^{(n)}$$
$$\boldsymbol{E}_z^{(n+1)} = \alpha\boldsymbol{E}_z^{\prime(n)} + (1-\alpha)\boldsymbol{E}_z^{(n)}$$

where $\boldsymbol{E}_z^{(n)}$ is the nth iterative approximation of $\boldsymbol{E}_z$ and α is a relaxation factor used to improve convergence. This can be rewritten as

$$\boldsymbol{E}_z^{(n+1)} = \left[(1-\alpha)\vec{\vec{I}} + \alpha\vec{\vec{K}}\vec{\vec{D}}\right]\boldsymbol{E}_z + \alpha\boldsymbol{E}_z^i. \quad (6)$$

This iterative scheme has the general form

$$\boldsymbol{x}^{(n+1)} = \vec{\vec{B}}\boldsymbol{x}^{(n)} + \boldsymbol{c}$$

of a stationary iterative method. It can be shown [15] that such an iterative method will converge for an arbitrary initial $\boldsymbol{x}^{(0)}$ if and only if

$$\rho(B) = \max_{1\le i\le n}|\lambda_i(\vec{\vec{B}})| < 1$$

where

$\rho(B)$ = spectral radius of $\vec{\vec{B}}$
$\lambda_i(B) = i^{\text{th}}$ eigenvalue of $\vec{\vec{B}}$.

This condition imposes a limit on the size parameter ka of the problems that can be solved by this iterative scheme. We have found that for the 2-D case of a 27.6-cm-diam cylinder with tissue dielectric properties corresponding to 100-percent muscle, this condition limits the convergence of (6) to frequencies less than 50 MHz for plane-wave illumination.

To alleviate this convergence problem, we have modified the method to implement a steepest descent iterative scheme described by Sarkar and Rao [12]. The iterative scheme for solving an equation of the form $\vec{\vec{A}}\boldsymbol{x} = \boldsymbol{y}$ is given by

$$\boldsymbol{x}^{(n+1)} = \boldsymbol{x}^{(n)} - \frac{\|\vec{\vec{A}}\boldsymbol{x}^{(n)} - \boldsymbol{y}\|^2}{\langle\vec{\vec{A}}\boldsymbol{x}^{(n)} - \boldsymbol{y}, \vec{\vec{A}}\left[\vec{\vec{A}}\boldsymbol{x}^{(n)} - \boldsymbol{y}\right]\rangle}\left[\vec{\vec{A}}\boldsymbol{x}^{(n)} - \boldsymbol{y}\right] \quad (7)$$

where, in our case

$$\vec{\vec{A}} = (\vec{\vec{I}} - \vec{\vec{K}}\vec{\vec{D}})$$
$$\boldsymbol{x}^{(n+1)} = \boldsymbol{E}_z^{(n+1)}$$
$$\boldsymbol{x}^{(n)} = \boldsymbol{E}_z^{(n)}$$
$$\boldsymbol{y} = \boldsymbol{E}_z^i.$$

The iterative scheme defined in (7) can be implemented by use of the convolution theorem in the manner previously described to compute (5) by (4) and the 2-D FFT algorithm. This modification of the K-space method extends the frequency limit of the 2-D problem described above to 500 MHz. Also, the number of iterations to converge the 50-MHz problem has reduced from 200 iterations for (6) to 10 iterations for (7), with 120 iterations required for the 500-MHz case. The computer time per iteration for (7) is approximately double that for (6).

III. Test Cases

To date, we have checked the procedure for the following three cases:

a) Homogeneous "infinite" cylindrical bodies of different permittivities, including those corresponding to 100-percent muscle [16], [17]. The fields incident on these bodies have been assumed to be due to plane waves or due to line sources in close proximity.

b) Layered "infinite" lossy cylindrical bodies with incident fields corresponding to those of plane wave or line sources.

c) An inhomogeneous body with the cross section corresponding to that containing the liver [18] for a human being (see Fig. 5).

As one of the cases for the category a) problems, a homogeneous, lossy, circular cylinder of diameter $2a = 27.6$ cm (approximate human girth) was considered. This problem can be solved analytically [10], which allows us to check the accuracy of the FFT approach. Figs. 1 and 2 compare the FFT results with the analytic solutions for a number of frequencies, from 40.68–433 MHz, with the dielectric constant and conductivity values taken as those of muscle tissue at the respective frequencies. The FFT results compare well with the analytic solutions.

For a test case representative of the layered bodies (category b) above), a two-layered cylinder is considered. The inner-layer radius is $a/2$ ($2a = 27.6$ cm). The dielectric constant for the outer layer is 10, with a conductivity of 0.1 S/m. The inner-layer dielectric constant and conductivity are double those of the outer layer. Figs. 3 and 4 compare the FFT versus analytic results at several frequencies. As with the homogeneous case, the FFT results agree favorably with the analytic solutions (maximum relative error ≤ 4 percent).

Finally, representative of the category c) problems, an inhomogeneous body with a cross section containing the liver of a human body has been considered. Fig. 5 shows the cross section and the 32×32 grid into which the model was discretized. The section was considered composed of seven types of tissues—skin, fat, muscle, bone, kidney, liver, and blood. A drawing of each of the tissue types was made on a transparency, which was then read into a 256×256 disk file by an optical-image digitizer. The files were then added together and a 32×32 file was created by averaging the 256×256 file over 8×8 blocks. The result of this procedure is that each square cell in the model contains the average complex permittivity within the corresponding cell of Fig. 5.

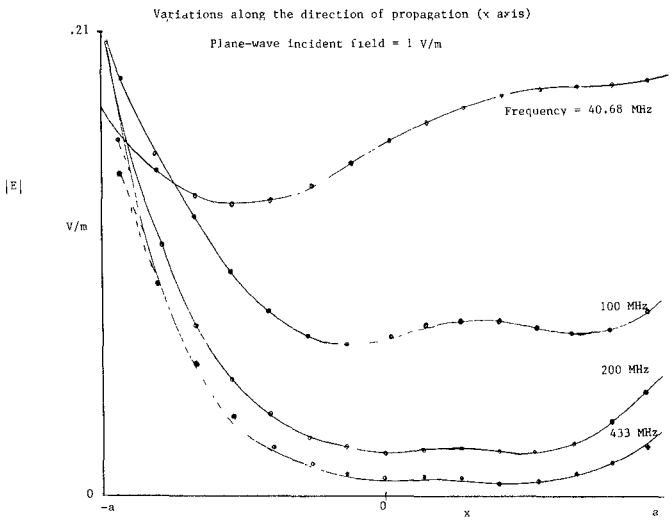

Fig. 1. Analytically calculated [10] internal E-field for a lossy homogeneous cylinder of radius $a = 13.8$ cm with dielectric properties of the muscle tissue [17]. The distributions calculated using the FFT approach are shown by dots.

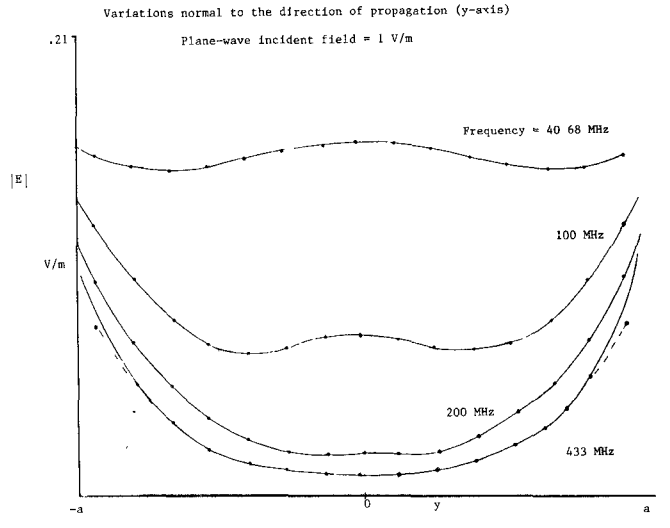

Fig. 2. Analytically calculated [10] internal E-field for a lossy homogeneous cylinder of radius $a = 13.8$ cm with dielectric properties of the muscle tissue [17]. The distributions calculated using the FFT approach are shown by dots.

The model was solved for a 110-MHz plane-wave incident field, and for the individual tissue permittivities given in Fig. 5. Sixty iterations were required to converge to the solution. A graph of the obtained SAR distribution is shown in Fig. 6. It may be noted that, as expected, there is definite reduction of SAR's in bone and fat. Also, a larger SAR is obtained for the frontal section of the body. An interesting point to note is the existence of high SAR's in regions of blood vessels and kidneys. This illustrates the ability of the FFT method to provide high-resolution SAR information.

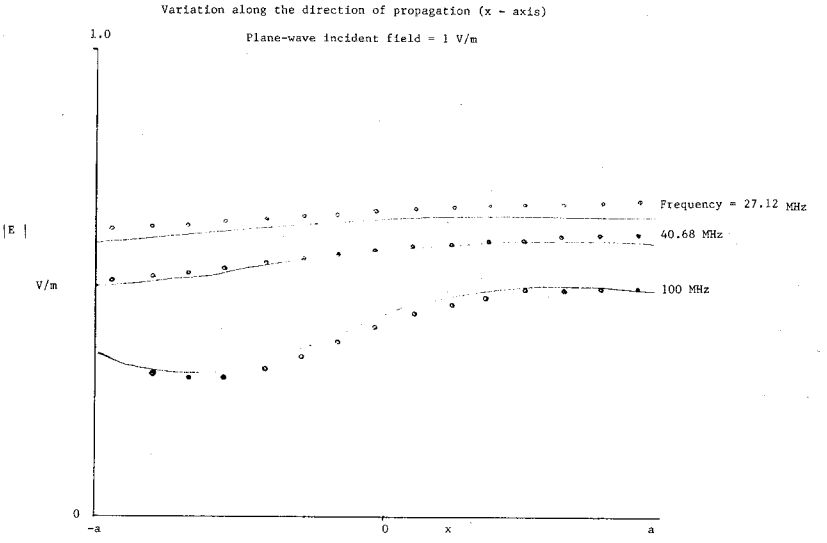

Fig. 3. Analytically calculated [10] internal E-field for a lossy, layered cylinder of outer radius $a = 13.8$ cm. For $0 < r < a/2$ $\epsilon_r = 20$, $\sigma = 0.2$ S/m, and for $a/2 < r < a$ $\epsilon_r = 10$, $\sigma = 0.1$ S/m. The distributions calculated using the FFT approach are shown by dots.

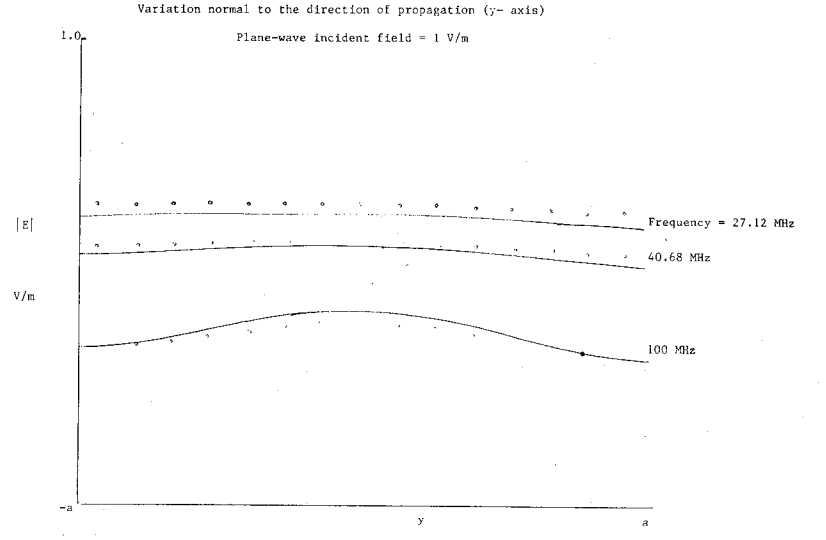

Fig. 4. Analytically calculated [10] internal E-field for a lossy, layered cylinder of outer radius $a = 13.8$ cm. For $0 < r < a/2$ $\epsilon_r = 20$, $\sigma = 0.2$ S/m, and for $a/2 < r < a$ $\epsilon_r = 10$, $\sigma = 0.1$ S/m. The distributions calculated using the FFT approach are shown by dots.

IV. Extension to 3-D Problems

It is planned to extend the FFT method to 3-D problems. Thus far, the only technique available to compute SAR distributions for models of man is the method of moments (MOM). Because the MOM involves solving a $3N \times 3N$ matrix equation (where N is the number of sample points), the number of operations needed to solve the problem increases rapidly (as N^2 to N^3), restricting therefore N to numbers on the order of 90–170 cells. Based on our experience with the FFT method, it appears feasible that this method could be used to solve 3-D problems for as many as 10^4 to 10^5 sample points in an acceptable period of time.

An obvious difficulty in solving man models with a large number of cells is the creation of the model (locations of the cells and their complex permittivities) itself. As an alternative to the hand-drawn sections for the various tissue types, we are experimenting with the use of a light pen to read the contours of the individual tissues for the various anatomical cross sections [18] of the human body directly into the computer. Another problem to be solved is the presentation of the results. Even though the isometric plots, such as Fig. 6, are useful, further refinements may lead to the use of a film writer to create grey-scale images where the grey-scale density of the films are proportional to the SAR's at the respective locations.

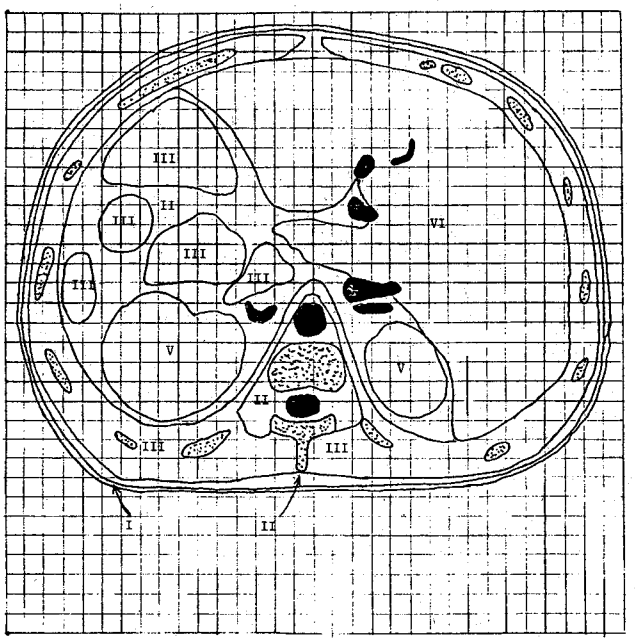

Tissue	ϵ_p	σ
I. Skin	75	1.19
II. Fat	8.6	0.071
III. Muscle	74	1.19
IV. Bone	8.6	0.071
V. Kidney	90	1.09
VI. Liver	80	.779
VII. Blood	77	2.1

Blood

Bone

Fig. 5. A seven-tissue model of a human cross section through the liver [18]. The dielectric properties were taken from [16].

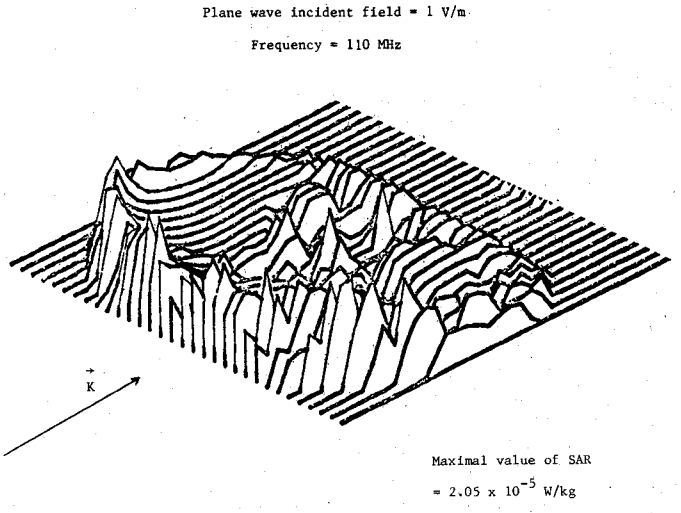

Fig. 6. Isometric plot of the FFT-calculated SAR distribution for the model of Fig. 5.

V. Conclusions

The paper presents a novel approach for calculating SAR distributions in arbitrary, lossy, dielectric bodies with a detail that has heretofore been impossible. To date, the method has been used for 2-D problems for which its accuracy has been confirmed by comparison with homogeneous and layered, circular, cylindrical bodies that have available analytic solutions. With computation times that are proportional to $N\log_2 N$ rather than N^2 to N^3 for the method of moments, the FFT approach should be extendable to 3-D bodies with 10 000 to 100 000 cells allowing, thereby, calculation of SAR's for the crucial regions such as the eyes and the gonads. Detailed distributions of SAR's are needed to assess biological effects of electromagnetic radiation.

Acknowledgment

The authors wish to thank the staff of the Diagnostic Imaging Laboratory of the University of Utah Radiology Department for the use of their Eclipse computer and image-processing software.

References

[1] O. P. Gandhi, "State of the knowledge for electromagnetic absorbed dose in man and animals," *Proc. IEEE*, vol. 68, pp. 24–32, Jan. 1980.

[2] C. H. Durney, "Electromagnetic dosimetry for models of humans and animals: A review of theoretical and numerical techniques," *Proc. IEEE*, vol. 68, pp. 33–40, Jan. 1980.

[3] I. Chatterjee, M. J. Hagmann, and O. P. Gandhi, "Electromagnetic energy deposition in an inhomogeneous block model of man for near-field irradiation conditions," *IEEE Trans. Microwave Theory Tech.*, vol. MTT-28, pp. 1452–1459, Dec. 1980.

[4] K. Karimullah, K. M. Chen, and D. P. Nyquist, "Electromagnetic coupling between a thin-wire antenna and a neighboring biological body: Theory and experiment," *IEEE Trans. Microwave Theory Tech.*, vol. MTT-28, pp. 1218–1225, Nov. 1980.

[5] C. H. Durney *et al.*, *Radio Frequency Radiation Dosimetry Handbook*, 3rd ed. Report SAM-TR-80-32 prepared for USAF School of Aerospace Medicine (AFSC), Brooks Air Force Base, Texas 78235, Aug. 1980.

[6] M. H. Repacholi, "Proposed exposure limits for microwave and radio-frequency radiations in Canada," *J. Microwave Power*, vol. 13, pp. 199–211.

[7] "1982: American National Standard Safety Levels with Respect to Human Exposure to Radiofrequency Electromagnetic Fields 300 kHz to 100 GHz," ANSI C95.1.

[8] K. M. Chen and B. S. Guru, "Internal EM field and absorbed power density in human torsos induced by 1–500 MHz EM Waves," *IEEE Trans. Microwave Theory Tech.*, vol. MTT-25, pp. 746–756, Sept. 1977.

[9] M. J. Hagmann, O. P. Gandhi, and C. H. Durney, "Numerical calculation of electromagnetic energy deposition for a realistic model of man," *IEEE Trans. Microwave Theory Tech.*, vol. MTT-27, pp. 804–809, Sept. 1979.

[10] H. Massoudi, *et al.*, "Electromagnetic absorption in multilayered cylindrical models of man," *IEEE Trans. Microwave Theory Tech.*, vol. MTT-27, pp. 825–829, Oct. 1979.

[11] N. N. Bojarski, "K-Space Formulation of the Electromagnetic Scattering Problem," Tech. Rep. AFAL-TR-71-5, Mar. 1971.

[12] T. K. Sarkar and S. M. Rao, "An iterative method for solving electrostatic problems," *IEEE Trans. Antennas Propagat.*, vol. AP-30, pp. 611–616, July 1982.

[13] J. H. Richmond, "Scattering by a dielectric cylinder—TM case," *IEEE Trans. Antennas Propagat.*, vol. AP-13, pp. 334–341, Mar. 1965.

[14] A. V. Oppenheim and R. W. Schafer, *Digital Signal Processing*. Englewood Cliffs, NJ: Prentice-Hall, 1975, pp. 110–111.

[15] D. Dahlquist, *Numerical Methods*. Englewood Cliffs, NJ: Prentice-Hall, 1974, p. 191.

[16] M. A. Stuchly and S. S. Stuchly, "Dielectric properties of biological substances—Tabulated," *J. Microwave Power*, vol. 15, pp. 19–26.

[17] C. C. Johnson and A. W. Guy, "Nonionizing electromagnetic wave effects in biological materials and systems," *Proc. IEEE*, vol. 60, pp. 692–718, June 1972.

[18] A. C. Eycleshymer and D. M. Shoemaker, *A Cross Section Anatomy*. New York: D. Appleton, 1911, p. 74.

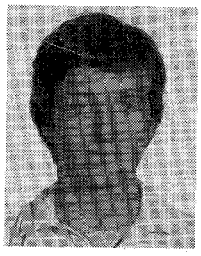

David T. Borup was born in Boise, ID, on October 24, 1958. He received the B.S. degree in mathematics from the College of Idaho, Caldwell, ID, in 1981. He is presently studying toward the Ph.D. degree at the University of Utah, Salt Lake City, where he has been working on numerical methods for microwave dosimetry.

✚

Om P. Gandhi (S'57–M'58–SM'65–F'79) received the B.Sc. (honors) degree in physics from Delhi University, Delhi, India, and the M.S.E. and Sc.D. degrees in electrical engineering from the University of Michigan, Ann Arbor.

He is a professor of Electrical Engineering at the University of Utah, Salt Lake City. He is an author or coauthor of one technical book and over 140 journal articles on microwave tubes, solid-state devices, and electromagnetic dosimetry and has recently written the textbook *Microwave Engineering and Applications* published by Pergamon Press. He has done pioneering work in quantifying the electromagnetic absorption in man and animals including the whole-body and part-body resonance conditions—work that formed an important basis for the new ANSI C95 recommended safety level with respect to human exposure to RF fields. He has been a principal investigator on over a dozen federally funded research projects since 1970, and serves or has served as a Consultant to several government agencies and private industries.

Dr. Gandhi received the Distinguished Research award of the University of Utah for 1979–1980 and a special award for "Outstanding Technical Achievement" from the Institute of Electrical and Electronics Engineers, Utah Section, in 1975. He edited a "*Proceedings of the IEEE*" Special Issue (January 1980) on Biological Effects and Medical Applications of Electromagnetic Energy. In addition to his membership on numerous national professional committees, he has been a Member of the Board of Directors of the Bioelectromagnetics Society and serves on the Editorial Board of its journal "Bioelectromagnetics." He is currently serving as the Chairman of the IEEE Committee on Man and Radiation (COMAR). His name is listed in *Who's Who in Engineering*, and *Who's Who in Technology Today*.

Characteristics of Transmission Lines with a Single Wire for a Multiwire Circuit Board

HISASHI SHIBATA AND RYUITI TERAKADO

Abstract—**This paper presents the characteristic impedance Z_0 and the phase velocity v_p of transmission lines with a single wire for a multiwire circuit board (MWB) under the quasi-TEM wave approximation. The characteristics are discussed for each of three investigated structures as: (I)$H = h + r$, (II)$H = h$, and (III)$H = h - r$, where r, h, and H are the radius of the wire, the thickness of the dielectric (adhesive layer), and the distance from the ground plane to the center of the wire, respectively. A charge simulation method is used for the calculation of the parameters. Z_0 and v_p are presented in graphical form for adhesive relative dielectric constants ϵ^* of 1.0, 2.65, and 5.0 as a function of r/h. An approximate formula of Z_0 for the structure of case (II) with $\epsilon^* = 5.0$ is also presented.**

I. Introduction

THE MULTIWIRE circuit board (MWB) [1]–[4] has become a center of attraction as a new technology for the printed wiring board. The technology is simple to design and offers the possibility of high interconnection density. The manufacturing process is described in [4]. The cross section of an MWB with a single wire is shown in Fig. 1. The electrical characteristics of the structure shown in Fig. 1 are discussed in [2], [3]. In general, the experiment based on the propagation delay [5] is used to obtain the characteristic impedance. Therefore, it is very important to present, theoretically, the design data for the impedance of the structure shown in Fig. 1.

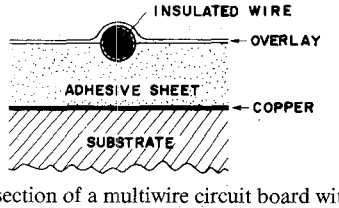

Fig. 1. Cross section of a multiwire circuit board with a single wire.

For this purpose, we consider three structures as shown in Fig. 2. The configurations of the structures are specified by the parameters r/h and H, where r, h, and H are the radius of the wire, the thickness of dielectric (adhesive) sheet, and the distance from the ground plane to the center of the wire, respectively. Because the coating of wire and the overlay in Fig. 2 have been neglected, the structures of Fig. 1 and Fig. 2(a) are different in a strict sense. However, when the thickness of the overlay is thin, the structure of Fig. 2(a) is, approximately, a good model for the analysis

Manuscript received April 22, 1983; revised November 2, 1983.

H. Shibata is with the Department of Electrical Engineering, Ibaraki Technical College, Katsuta, Ibaraki, 312 Japan.

R. Terakado is with the Department of Electrical Engineering, Faculty of Engineering, Ibaraki University, Hitachi, Ibaraki, 316 Japan.

0018-9480/84/0400-0360$01.00 ©1984 IEEE